Molecular and Cellular Biology

Plk1 Phosphorylates Sgt1 at the Kinetochores To Promote Timely Kinetochore-Microtubule Attachment

X. Shawn Liu, Bing Song, Jiabin Tang, Weiyi Liu, Shihuan Kuang and Xiaoqi Liu

---

Updated information and services can be found at:
http://mcb.asm.org/content/32/19/4053

These include:

SUPPLEMENTAL MATERIAL

http://mcb.asm.org/content/suppl/2012/09/06/MCB.00516-12.DCSupplemental.html

REFERENCES

This article cites 42 articles, 17 of which can be accessed free at: http://mcb.asm.org/content/32/19/4053#ref-list-1

CONTENT ALERTS

Receive: RSS Feeds, eTOCs, free email alerts (when new articles cite this article), more»

Information about commercial reprint orders: http://journals.asm.org/site/misc/reprints.xhtml
To subscribe to to another ASM Journal go to: http://journals.asm.org/site/subscriptions/

Journals.ASM.org

Plk1 Phosphorylates Sgt1 at the Kinetochores To Promote Timely Kinetochore-Microtubule Attachment

X. Shawn Liu,[a,c] Bing Song,[b,c] Jiabin Tang,[a] Weiyi Liu,[d] Shihuan Kuang,[d] and Xiaoqi Liu[a,c]

Department of Biochemistry,[a] Department of Biological Sciences,[b] Center for Cancer Research,[c] and Department of Animal Sciences,[d] Purdue University, West Lafayette, Indiana, USA

Accurate chromosome segregation during cell division maintains genomic integrity and requires the proper establishment of kinetochore-microtubule attachment in mitosis. As a key regulator of mitosis, Polo-like kinase 1 (Plk1) is essential for this attachment process, but the molecular mechanism remains elusive. Here we identify Sgt1, a cochaperone for Hsp90, as a novel Plk1 substrate during mitosis. We show that Sgt1 dynamically localizes at the kinetochores, which lack microtubule attachments during prometaphase. Plk1 is required for the kinetochore localization of Sgt1 and phosphorylates serine 331 of Sgt1 at the kinetochores. This phosphorylation event enhances the association of the Hsp90-Sgt1 chaperone with the MIS12 complex to stabilize this complex at the kinetochores and thus coordinates the recruitment of the NDC80 complex to form efficient microtubule-binding sites. Disruption of Sgt1 phosphorylation reduces the MIS12 and NDC80 complexes at the kinetochores, impairs stable microtubule attachment, and eventually results in chromosome misalignment to delay the anaphase onset. Our results demonstrate a mechanism for Plk1 in promoting kinetochore-microtubule attachment to ensure chromosome stability.

Chromosome segregation errors during mitosis can result in genomic instability, which is a major driving factor for tumorigenesis. Accurate chromosome segregation requires the assembly of mitotic kinetochores on centromeric chromatin to mediate its interaction with spindle microtubules. The human kinetochore is a multilayered disk structure that contains more than 100 protein components (5, 42). The inner kinetochore consists of proteins constitutively present at centromeres during the cell cycle, known as CCAN, the constitutive centromere-associated network (10, 16). Distinguished from CCAN, outer kinetochore proteins accumulate at kinetochores beginning at prophase. Among them, the KMN network, including the KNL1 protein, the MIS12 complex, and the NDC80 complex, produces core attachment sites for spindle microtubules (6, 40). Extended from the outer kinetochore is a dense array of fibers, the fibrous corona, where the spindle assembly checkpoint (SAC) monitors correct kinetochore-microtubule attachment (31).

Polo-like kinase 1 (Plk1) plays a vital role during mitosis. Enriched on critical mitotic structures, including centrosomes, kinetochores, and midbodies, Plk1 is involved in almost every step of mitosis (4, 37). Accumulating evidence suggests that Plk1 is required for the establishment and maintenance of stable kinetochore-microtubule attachment (23, 38). Several kinetochore proteins, such as INCENP (12), NudC (32), PBIP (19), and Bub1 (34), have been reported to recruit Plk1 at the kinetochores. However, if and how Plk1 directly regulates the kinetochore-microtubule attachment are unclear.

Sgt1, originally identified as a suppressor of the G_2 allele of SKP1 in *Saccharomyces cerevisiae* (21), conservatively functions as a cochaperone for Hsp90 in kinetochore assembly throughout eukaryotes (2, 8, 24, 35). Here we demonstrate that Sgt1 dynamically localizes at the kinetochores, which lack microtubule attachments during prometaphase. Plk1 is required for the kinetochore localization of Sgt1 and phosphorylates Sgt1 at the kinetochores. This phosphorylation event enhances the association of Sgt1 with Dsn1, one component of the MIS12 complex, and thus facilitates the kinetochore localization of this complex. Disruption of Sgt1

phosphorylation reduced the MIS12 and NDC80 complexes at kinetochores and resulted in the impairment of stable kinetochore-microtubule attachment, chromosome misalignment, and the delay of anaphase onset. These results suggest a novel mechanism for Plk1 function in the regulation of kinetochore-microtubule attachment.

MATERIALS AND METHODS

Cell culture, RNA interference (RNAi), constructs, and transfection. HeLa cells and HEK 293T cells were cultured in Dulbecco modified Eagle medium (DMEM) supplemented with 10% fetal bovine serum, 100 units/ml penicillin, and 100 units/ml streptomycin at 37°C in 5% CO_2. Human Sgt1 small interfering RNA (siRNA; 5′-AAGGCUUUGGAACAG AAACCA-3′) was obtained from Dharmacon (36). Plk1 siRNA (5′-AAG GCGGCUUUGCCAAGTGCTT-3′) was from Dharmacon (25). Double-stranded siRNA was transfected with Oligofectamine reagent (Invitrogen) and plasmid DNA was transfected with MegaTran (Origene) as described by the manufacturers. Yellow fluorescent protein (YFP)-hDsn1 and YFP-hNsl1 constructs were gifts from Iain Cheeseman (MIT).

***In vitro* kinase assay.** Various glutathione *S*-transferase (GST)-tagged murine Sgt1 constructs were subcloned into pGEX-KG, expressed in *Escherichia coli*, and purified. Point mutations were generated by use of the QuikChange site-directed mutagenesis kit (Stratagene). Purified recombinant Sgt1 was incubated with purified Plk1 in kinase reaction buffer (50 mM Tris [pH 7.5], 10 mM $MgCl_2$, 2 mM EGTA, 0.5 mM sodium vanadate, 100 mM *p*-nitrophenylphosphate, 25 mM dithiothreitol, 125 mM ATP) supplemented with 10 μCi of [γ-^{32}P]ATP at 30°C for 30 min. The reaction mixtures were resolved by SDS-PAGE, stained with Coomassie brilliant blue (CBB), dried, and subjected to autoradiography.

Antibodies. The antibody against human Sgt1 was generated by Proteintech (Chicago, IL). This polyclonal antibody was affinity purified from immunized rabbits and recognizes the sequence in the SGS domain of Sgt1 (EVKRAMNKSFMESGGTV). The phospho-specific antibody against pS331 of human Sgt1 was also generated by Proteintech. Briefly, a peptide containing phospho-S331 (EVKRAMNKS$_p$FMESGGTV) was synthesized and used to immunize rabbits. After the antibodies were affinity purified, a series of control experiments was performed to confirm its specificity. Anti-Dsn1, anti-Nsl1, and anti-Nnf1 antibodies were gifts from Arshad Desai (UCSF). We also purchased the following antibodies: anti-Sgt1 (612104; Becton, Dickinson [BD]), anti-Plk1 (sc-17783; Santa Cruz Biotechnology), human anticentromere antibody (ACA; Antibodies Incorporated), anti-Mis12 (A300-776A; Bethyl), anti-Mad2 (ab24588; Abcam), anti-α-tubulin (T-6557; Sigma), anti-β-actin (A-5441; Sigma), anti-Flag (F-3165; Sigma), anti-green fluorescent protein (anti-GFP; A11122; Invitrogen), and anti-phospho-histone H3 (06-570; Millipore).

IP. Whole-cell lysates were incubated with various antibodies as indicated for each experiment for 1 h at 4°C, followed by 1-h incubation with protein A/G-Sepharose beads. After immunocomplexes were resolved by SDS-PAGE, coimmunoprecipitated (co-IP) proteins were detected by Western blotting with antibodies as indicated for the specific experiments.

Immunofluorescence and image quantification. For immunofluorescence (IF) and image quantification, cells were grown on coverslips under the culture conditions described above, treated with PHEM buffer [60 mM piperazine-N,N'-bis(2-ethanesulfonic acid), 25 mM HEPES, 10 mM EGTA, and 2 mM MgCl$_2$; pH 6.9] plus 1% Triton X-100 for 5 min, fixed in PHEM buffer with 4% formaldehyde, and blocked in phosphate-buffered saline with 5% bovine serum albumin and 0.1% Triton X-100 for 1 h. Primary and secondary antibody incubations were conducted for 1 h at room temperature. For cold-stable kinetochore fiber analysis, cells were incubated on ice for the indicated times, then fixed for 10 min on ice, followed by 10 min at room temperature with PHEM buffer containing 4% formaldehyde and 0.2% Triton X-100 (22). Cells were then processed as described above. Goat anti-mouse IgG–Alexa Fluor 594, 498, or 688 (Invitrogen) or goat anti-rabbit IgG–Alexa Fluor 594 or 498 (Invitrogen) was used at 1:200 dilutions. IF images were collected at room temperature with a Nikon C1+ microscope equipped with a 60×, 1.4 numerical aperture oil immersion lens. Measurements of kinetochore intensities were conducted with maximum intensity projections of images. Kinetochore exposure settings were held constant within each group of experiments, and kinetochore signals within each figure are scaled equally. Maximal kinetochore intensities and corresponding background levels were measured from radial 7-by-7-pixel areas for each kinetochore focus, using ImageJ. Minima of 5 cells and 20 kinetochore foci per cell were measured for each condition (each experiment was replicated a minimum of three times). Kinetochore focus intensities were then pooled within a given experiment, and the mean kinetochore fluorescence intensity was calculated. Statistical significance was evaluated by using a two-tailed Student t test, and results with P values of <0.05 were considered statistically significant. The correlation between Sgt1 signal and Plk1 signal at individual kinetochores was measured by Pearson product-moment correlation coefficient analysis, and a Pearson product-moment correlation coefficient (r) of >0.9 was considered highly linear correlation.

Time-lapse video microscopy for live cells. HeLa cells only expressing Flag–Sgt1-WT, -S302Am, or -S302E were used for time-lapse video microscropy of live cells. Image acquisition was performed with a Nikon A1R microscope equipped with a 20× lens and enclosed in a chamber to maintain temperature for live cells. During filming, cells were maintained in HEPES-buffered DMEM at 37°C. After treatment with Hoechst 33342, cells were tracked for 5 h, and images were acquired at 7-min intervals with Nikon software.

RESULTS

Sgt1 dynamically localizes at the kinetochores during mitosis.
To explore Sgt1 function, we developed a polyclonal antibody

against Sgt1 to study its subcellular localization. By using this antibody in IF staining, we found that Sgt1 displayed a diffuse pattern in paraformaldehyde-fixed HeLa cells during mitosis (Fig. 1A), consistent with the previous report of Sgt1 as a highly soluble protein (36). In order to rigorously test whether Sgt1 associates with any specific subcellular structure, cells were extracted with the PHEM buffer containing detergent (1% Triton X-100) before fixation with paraformaldehyde (see Materials and Methods). We then observed that Sgt1 was present as dots in variable numbers and staining intensities during prometaphase. Significantly, these dots colocalized with centromeres, suggesting that Sgt1 is recruited at the kinetochores. The number of dots decreased as the cell proceeded from prometaphase to metaphase, whereas no dots colocalizing with centromeres were detected in either prophase or metaphase (Fig. 1B).

As kinetochore-microtubule attachment is being established during prometaphase, it is possible that kinetochore localization of Sgt1 is determined by the presence or absence of microtubules at kinetochores. To test this hypothesis, we treated cells with nocodazole to disrupt microtubules, or with paclitaxel (originally named taxol) to stabilize microtubules and then examined Sgt1 localization by IF staining. Upon nocodazole treatment, all the kinetochores were strongly labeled by Sgt1. In contrast, Sgt1 was not present at kinetochores after paclitaxel treatment (Fig. 1C). These data suggest that Sgt1 is recruited to the kinetochores that lack microtubule attachments. In a second approach to test our hypothesis, Sgt1 localization was examined in cells treated with monastrol, which does not interfere with microtubule dynamics. Cells form monopolar spindles after monastrol treatment (28). In these cells, Sgt1 only localized at the kinetochores lacking microtubule attachments, but not at the kinetochores with microtubules (Fig. 1D), further confirming that Sgt1 specifically localizes at unattached kinetochores.

To validate the specificity of this anti-Sgt1 antibody, we first applied RNAi to deplete endogenous Sgt1 in HeLa cells. In immunoblot analysis, this antibody recognized a doublet from lysates of control HeLa cells, corresponding to two splicing isoforms of Sgt1, but not from lysates of Sgt1-depleted cells (Fig. 1E, right panel). In IF staining experiments with this antibody, previously observed kinetochore foci were undetectable after Sgt1 RNAi upon nocodazole treatment (Fig. 1E, left panel), suggesting that the kinetochore dots stained by this antibody represented bona fide Sgt1 signals. Further, this antibody detected Sgt1 at the kinetochores in multiple cell lines (Fig. 1F), including several cancer cell lines, such as U2OS (a human osteosarcoma cell line), PC-3 (a human prostate cancer cell line), and MCF-7 (a human breast cancer cell line), and nontransformed cells, such as RWPE-1 (an immortalized human prostate cell line). Besides the Sgt1 staining observed with this antibody, we also generated a U2OS cell line that stably expressed GFP-Sgt1, and with it we were able to detect GFP-Sgt1 at the kinetochores after nocodazole treatment (Fig. 1G). Taking these observations together, we conclude that Sgt1 dynamically localizes at the kinetochores that lack microtubule attachments during prometaphase.

Plk1 phosphorylates Sgt1 at serine 331. Proteomic screening identified Sgt1 as an interacting partner of Plk1 during mitosis (26). We were able to detect the interaction between Sgt1 and Plk1 in both overexpressed proteins (Fig. 2B) and endogenous proteins (Fig. 2A). Moreover, purified GST-Sgt1 was able to pull down Plk1 from mitotic cell extracts (Fig. 2C).
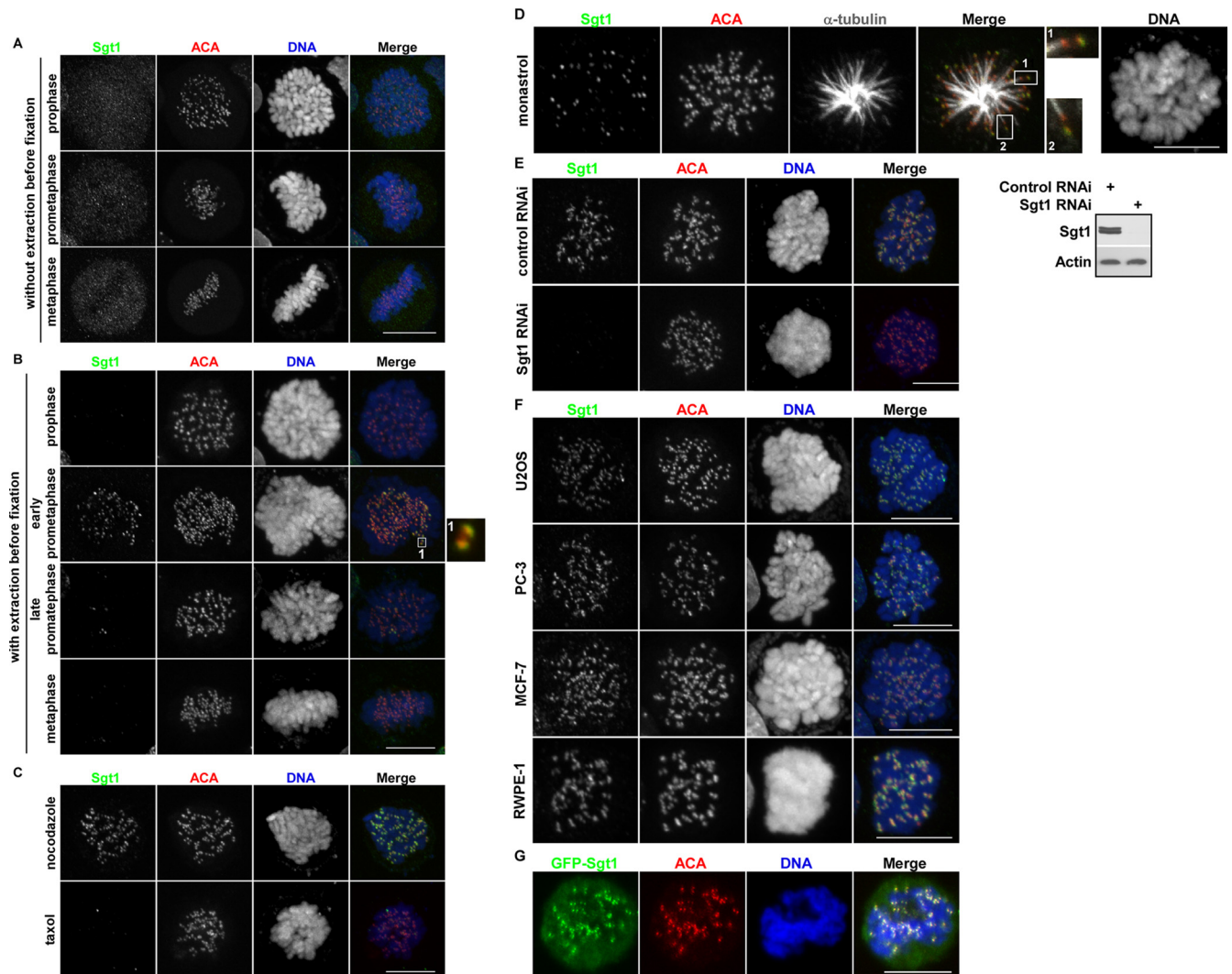
FIG 1 Sgt1 dynamically localizes at the kinetochore during mitosis. (A and B) HeLa cells in various mitotic stages were directly fixed in 4% paraformaldehyde (A) or extracted by 1% Triton X-100 treatment (B) and then stained for IF with anti-Sgt1 antibody or ACA and with 4′,6-diamidino-2-phenylindole (DAPI). Individual and merged fluorescent images are presented. An enlarged image on the right shows that Sgt1 (green) colocalizes with the centromere (red). Bar, 10 μm. (C) HeLa cells were treated with 1 μM nocodazole or 1 μM paclitaxel for 2 h and then subjected to IF staining as described for panel B. Bar, 10 μm. (D) HeLa cells were treated with 68 μM monastrol for 2 h and processed for IF staining with anti-Sgt1, ACA, or anti-α-tubulin antibodies and then DAPI. Two enlarged images (boxes 1 and 2) on the right of the merged image show that single kinetochores with microtubule attachment do not show Sgt1 staining, whereas other kinetochores lacking microtubule attachment show positive Sgt1 staining. Bar, 10 μm. (E) HeLa cells were transfected with control or Sgt1 siRNAs for 72 h and subjected to immunoblotting (right panel) or IF staining (left panel) with the indicated antibodies. Nocodazole was added 2 h before the cells were harvested for IF staining. Bar, 10 μm. (F) U2OS, PC-3, MCF-7, and RWPE-1 cells were treated as described for panel B. Nocodazole was added to these cells before they were subjected to anti-Sgt1 IF staining. Bar, 10 μm. (G) U2OS cells were transfected with GFP-Sgt1 and selected by use of G418 for 2 weeks. Cells were treated with nocodazole and subjected to IF staining with anti-GFP antibody and ACA. Bar, 10 μm.

Next we asked whether Sgt1 is a substrate of Plk1. In an *in vitro* kinase assay, murine Sgt1 amino acids 161 to 336 served as a robust substrate for Plk1 (Fig. 2D). Subsequently, serine 302 of murine Sgt1 (corresponding to serine 331 of human Sgt1) was identified as the Plk1 phosphorylation site *in vitro* by site-directed mutagenesis (Fig. 2E and F). To test whether Sgt1 is phosphorylated by Plk1 in cells, a polyclonal antibody directed against a peptide encompassing phosphoserine 331 of human Sgt1 (p-Sgt1) was generated (see Materials and Methods). After incubation with Plk1, only wild-type murine Sgt1 (Sgt1-wt), but not S302A, was recognized by the p-Sgt1 antibody, suggesting that serine 302 of murine Sgt1 is directly phosphorylated by Plk1 *in*

vitro (Fig. 2G). Moreover, murine Sgt1-wt, but not S302A, expressed in HEK 293T cells was recognized by the p-Sgt1 antibody (Fig. 2H), indicating that the phosphorylation event occurs in cells. The p-Sgt1 epitope was lost upon phosphatase treatment of lysates from cells expressing GFP–Sgt1-wt, confirming the specificity of this antibody for phosphorylated Sgt1 (Fig. 2I). Most importantly, the p-Sgt1 antibody identified the phosphorylated form of human Sgt1, including two isoforms in lysates from HeLa cells treated with nocodazole but not from Plk1-depleted cells (Fig. 2J) or from Plk1-inhibited cells (treated with BI 2536) (Fig. 2K), suggesting that endogenous human Sgt1 is phosphorylated at serine 331 in a Plk1-dependent manner. The surrounding sequence of
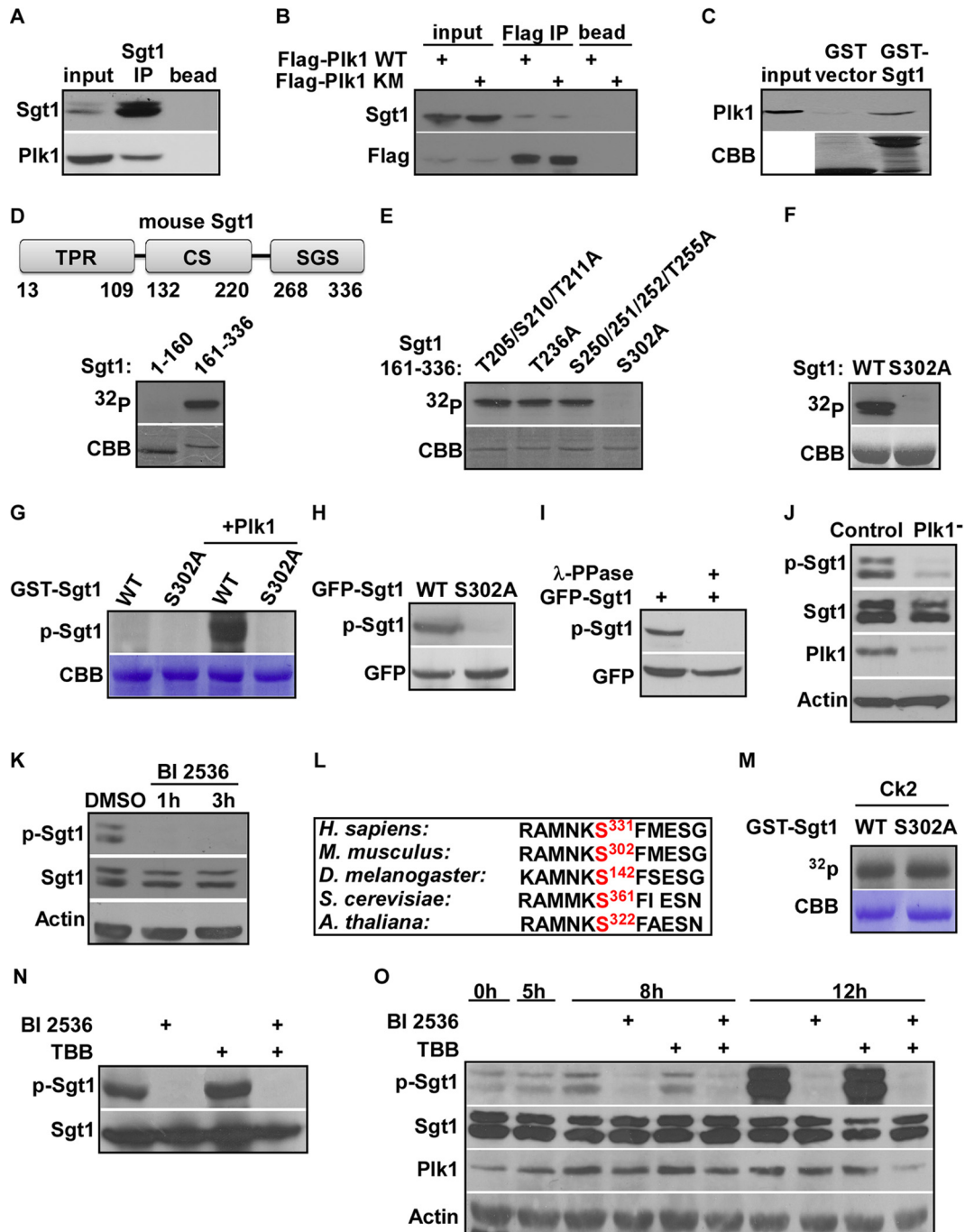
FIG 2 Plk1 phosphorylates Sgt1 at serine 331. (A) HeLa cells were treated with nocodazole for 8 h and harvested for IP with anti-Sgt1 antibody, followed by Western blot (WB) analysis. (B) HEK 293T cells were transfected with GFP-Sgt1 or Flag-Plk1 wild type (WT) or K82M (KM; kinase-dead mutant), treated with nocodazole for 8 h, and harvested for IP with anti-Flag antibody, followed by WB analysis. (C) Purified GST-Sgt1 or GST proteins bound on glutathione beads were incubated with mitotic cell extracts prepared from nocodazole-treated HeLa cells. The reaction mixture was resolved by SDS-PAGE, followed by WB. The bottom panel shows CBB staining results. (D to K) Plk1 phosphorylates human Sgt1 at serine 331 *in vitro* and *in vivo*. (D, upper panel) Schematic representation of mouse Sgt1. TPR, tetratricopeptide repeat domain; CS, Chord- and Sgt1-specific domain; SGS, Sgt1-specific domain. (Lower panel) Purified fragments of murine Sgt1 (amino acids 1 to 160 and 161 to 336) were incubated with Plk1 in the presence of [γ-^{32}P]ATP. Then, the reaction mixture was resolved by SDS-PAGE, stained with CBB, and proteins were detected by autoradiography. (E) The indicated forms of murine GST–Sgt1-161-336 were subjected to an *in vitro* Plk1 kinase assay as described for panel D. (F) Purified murine full-length GST–Sgt1-WT or -S302A was subjected to an *in vitro* Plk1 kinase assay as for panel D. (G) Purified murine GST–Sgt1-WT or -S302A was incubated with or without Plk1 in the presence of unlabeled ATP. Then, the reaction mixture was resolved by SDS-PAGE, followed by WB with an antibody raised against the human Sgt1 peptide containing phosphorylated S331, the site corresponding to murine S302. (H) HEK 293T cells were transfected with murine Sgt1 constructs (GFP–Sgt1-WT or -S302A) and treated with nocodazole, followed by WB. (I) Cell extracts prepared as for panel H were treated with λ-phosphatase, followed by WB. (J) HeLa cells were depleted of Plk1 with siRNA, treated with nocodazole, and harvested for WB analysis. (K) HeLa cells were treated with 100 nM BI 2536 or the carrier (dimethyl sulfoxide [DMSO]) for 1 h or 3 h and harvested for WB analysis. (L) Alignment of Sgt1 protein sequences containing the equivalent of serine 331 in different species. (M) Purified murine GST-Sgt1 (WT or S302A) was subjected to an *in vitro* Ck2 kinase assay as for panel D. (N) HEK 293T cells were transfected with GFP-Sgt1. After transfection, cells were treated with BI2536, TBB (a Ck2 inhibitor), or both drugs for 12 h, and then harvested for WB analysis. (O) HeLa cells were synchronized with a double thymidine block (DTB; 16 h of treatment with thymidine, 8 h of release, and a second 16-h block with thymidine) at the G$_1$/S boundary. After release from the second block for 5 h, cells were treated with BI2536, TBB, or both drugs for an additional 3 h or 7 h and then harvested for WB analysis.
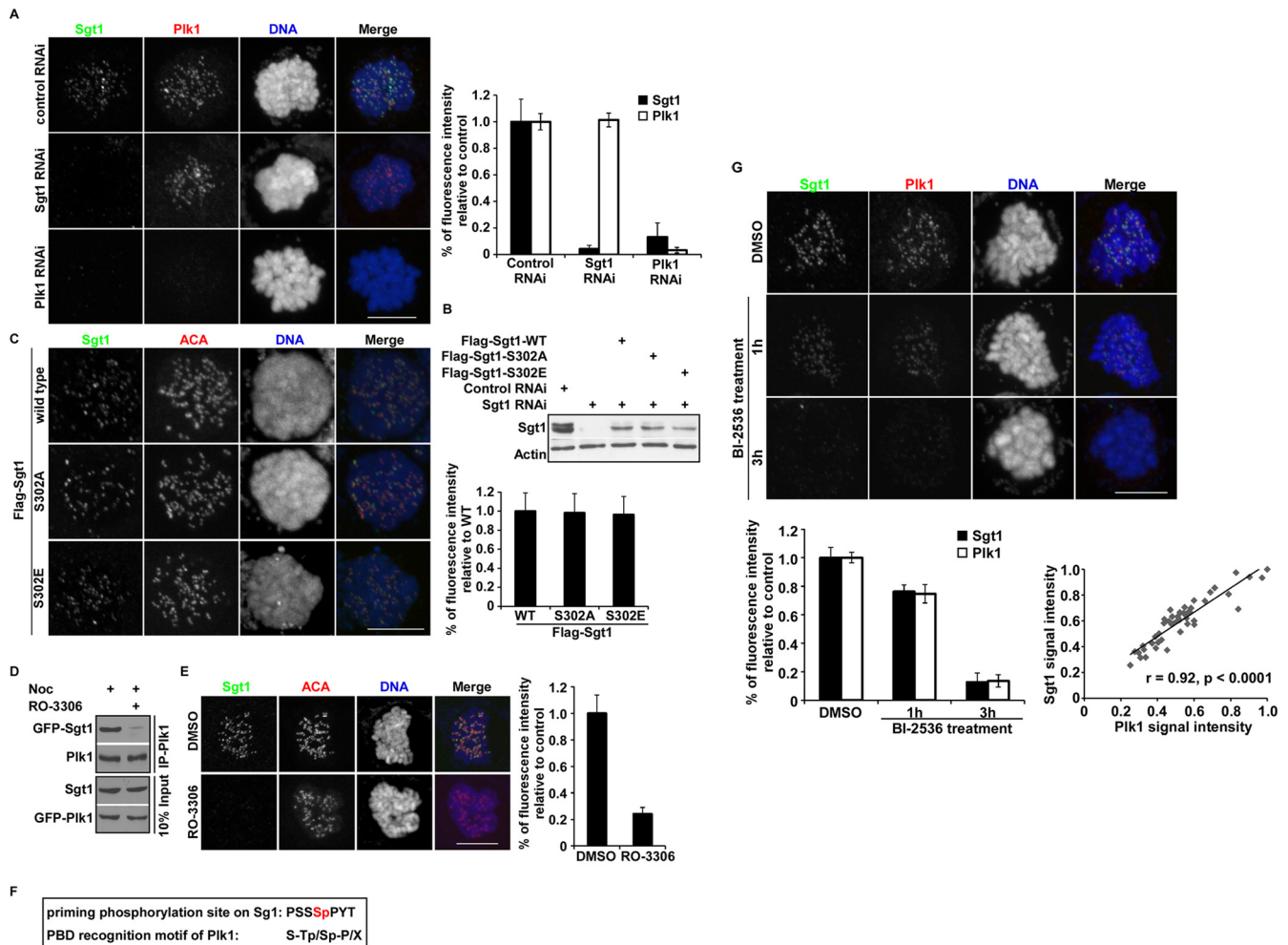
FIG 3 Plk1 is required for Sgt1 localization at the kinetochore. (A) HeLa cells were transfected with control, Sgt1, or Plk1 siRNAs, treated with nocodazole, and processed for IF staining with antibodies against Sgt1 or Plk1. Bar, 10 μm. Fluorescence signals of Sgt1 and Plk1 at kinetochores were quantified using ImageJ (see Materials and Methods) after each RNAi treatment. For each sample, a mean of multiple kinetochores from 5 cells was used to calculate the mean values; error bars represent the deviations from the means observed in multiple cells. The mean fluorescence intensities for control RNAi cells were set to 100%, and the fraction of signal remaining after Sgt1 or Plk1 RNAi treatment was calculated. The trend was observed in three repeats of the experiment. (B) HeLa cells were transfected with control or Sgt1 siRNAs alone or with Sgt1 siRNA together with murine Flag-Sgt1 constructs (WT, S302A, or S302E) for 72 h and then harvested for WB analysis. (C) The cells shown in panel B were treated with nocodazole and processed for IF staining. Fluorescence signals of Sgt1 at kinetochores in each cell were quantified as for panel A. Bar, 10 μm. (D) HEK 293T cells were transfected with GFP-Sgt1, treated with dimethyl sulfoxide (DMSO) or 1 μM RO-3306, a Cdk1 inhibitor (39), for 1 h in the presence of nocodazole, and harvested for IP with anti-Plk1 antibody, followed by WB analysis. (E) HeLa cells were treated with DMSO or 1 μM RO-3306 for 1 h in the presence of nocodazole and processed for IF staining. Bar, 10 μm. (F) The priming phosphorylation site of Sgt1 fits the PBD recognition motif of Plk1. (G) HeLa cells were treated with DMSO or 100 nM BI 2536 for 1 h or 3 h and processed for IF staining. Nocodazole was added 0.5 h before harvest. The upper panel shows representative images. In the lower left panel, fluorescence signals of Sgt1 and Plk1 at kinetochores after each treatment were quantified as for panel A. In the lower right panel, the correlation between Sgt1 signal and Plk1 signal at individual kinetochores in BI 2536-treated cells for 1 h was measured by Pearson correlation coefficient analysis ($r = 0.92 \pm 0.02$; $P < 0.001$; $n > 50$ cells); the signal intensities of Plk1 and Sgt1 within a single cell are shown as the percentages of the highest intensity in the respective cell.

serine 331 fit the newly defined Plk1 consensus phosphorylation motif: [D/N/E]-X-S/T-[F/Φ; no P]-[Φ/X] (1, 20). Serine 331 is highly conserved across species (Fig. 2L), indicating a potential functional significance. Therefore, we used murine Sgt1 to generate various constructs (WT, S302A, S302E) for use in further experiments, as these constructs, when expressed in human cells, are RNAi resistant. It has been reported that budding yeast Sgt1 is phosphorylated at serine 361 by Ck2 (3); however, Ck2 is not responsible for phosphorylation of serine 331 on human Sgt1 (Fig. 2M to O).

Plk1 is required for Sgt1 localization to unattached kinetochores. Plk1 is detected at centromeres in the G_2 phase and en-

riches at kinetochores during prometaphase (33). We asked whether kinetochore localization of Sgt1 is affected by Plk1 or vice versa. As shown in Fig. 3A, the Sgt1 signal was reduced to 10% compared to control RNAi cells after Plk1 depletion, whereas Sgt1 depletion exerted no notable effect on kinetochore localization of Plk1. These data suggest that Plk1 is required for Sgt1 to localize at the kinetochores. To understand how Sgt1 is recruited at the kinetochores by Plk1, we first tested whether phosphorylation of Sgt1 is required for its kinetochore localization; endogenous Sgt1 was replaced with murine Flag-Sgt1 wild type (WT), S302A (unphosphorylatable mutant), or S302E (phosphorylation-mimick-

ing mutant) by cotransfection of HeLa cells with Sgt1 siRNA and the Flag-Sgt1 constructs mentioned above. The replacing efficiency was examined by immunoblot analysis (Fig. 3B). Both Sgt1-WT- and Sgt1-S302A-expressing cells showed comparable levels of Sgt1 signals at kinetochores after nocodazole treatment (Fig. 3C), suggesting that Plk1-mediated phosphorylation of Sgt1 is not required for its kinetochore localization. It has been established that the Polo-box domain of Plk1 mediates its binding to its substrates and that this binding is often dependent on the initial phosphorylation by a priming kinase, such as Cdk1, to generate a docking site (S-Sp/Tp-P/X) for the Polo-box domain to recognize (4). Since Sgt1 was identified as a Polo-box domain-interacting protein (26) and was reported to be phosphorylated by Cdk1 (15), we next tested whether Plk1 binding to Sgt1 is regulated by Cdk1 phosphorylation. As shown in Fig. 3D, inhibition of Cdk1 kinase activity reduced the binding between Plk1 and Sgt1. Moreover, Sgt1 kinetochore localization was abolished after Cdk1 inhibition (Fig. 3E). The priming phosphorylation site of Sgt1 fits the PBD recognition motif (Fig. 3F). These data suggest that recruitment of Sgt1 at the kinetochores by Plk1 depends on the priming phosphorylation of Sgt1 by Cdk1 but not the phosphorylation by Plk1. Further, when cells were treated with BI 2536, which was able to decrease Plk1 kinetochore localization (23), we observed that the level of Sgt1 was proportional to that of diminished Plk1 at kinetochores under BI 2536 treatment (Fig. 3G). Taken together, these data support the notion that Plk1 is required for Sgt1 kinetochore localization in a kinase activity-independent manner.

Temporal and spatial regulation of Sgt1 phosphorylation at serine 331. Next, we used the p-Sgt1 antibody to characterize the temporal and spatial regulation of this phosphorylation event. As shown in Fig. 4A, phosphorylation of serine 331 was detected at 8 h after release from thymidine block, decreased at 13 h, and peaked in nocodazole-treated cells. Generation of the p-Sgt1 epitope correlated with the activity level of Plk1, which peaks in prometaphase (11). Thus, these data suggest that Sgt1 is mainly phosphorylated during prometaphase. To examine the dephosphorylation of Sgt1, cells were enriched at prometaphase by nocodazole treatment and released into fresh medium for different time periods. Dephosphorylation of serine 331 occurred slightly later than dephosphorylation of histone H3 (Fig. 4B), which begins from anaphase (14), suggesting that dephosphorylation of serine 331 likely occurs at the end of mitosis. In short, we found that Sgt1 is phosphorylated at serine 331, predominantly during prometaphase.

The phospho-specific antibody was then used to examine the subcellular localization of the phosphorylated form of Sgt1 by using IF staining. Consistent with the results obtained by immunoblotting, phosphorylation of Sgt1 was mainly observed in prometaphase and was present as dots that colocalized with centromeres (Fig. 4C). Overall phosphorylation of Sgt1 was very low in prophase, and no phosphorylation of Sgt1 at kinetochores was detected in metaphase cells. To validate the specificity of this antibody in IF staining, endogenous Sgt1 was depleted by RNAi, and the phosphorylation signal at kinetochores in prometaphase cells was abolished (Fig. 4D), suggesting that kinetochore dots detected by this antibody in IF staining represent Sgt1 signal. Moreover, when the cells were treated with BI 2536 for a short period (1 h), the phosphorylation signal of Sgt1 at kinetochores was also abolished (Fig. 4E), indicating that Sgt1 at kinetochores is phosphorylated by Plk1. To test whether kinetochore localization of Sgt1 is

a prerequisite step for its phosphorylation at kinetochores, we compared the phosphorylation level of Sgt1 upon nocodazole treatment with paclitaxel treatment, as Sgt1 is recruited at the kinetochores by nocodazole treatment but not paclitaxel treatment (Fig. 1C). As shown in Fig. 4F, Sgt1 phosphorylation was significantly induced by nocodazole treatment but not by paclitaxel treatment. Thus, these data suggest that Plk1 phosphorylates Sgt1 at kinetochores predominantly during prometaphase, when kinetochore-microtubule attachment is being established.

Phosphorylation of Sgt1 is required for proper mitotic progression. We next sought to define the contribution of this mitotic phosphorylation event. Endogenous Sgt1 was replaced with murine Flag-Sgt1 constructs (WT, S302A, or S302E) in HeLa cells and then subjected to time-lapse imaging to follow mitotic progression. As shown in Fig. 5A, from chromosome condensation to decondensation, cells expressing Flag–Sgt1-WT completed mitosis within 60 min, whereas cells expressing Sgt1-S302A required 120 min and cells expressing Flag–Sgt1-S302E needed 85 min. In particular, anaphase onset in Sgt1-S302A-expressing cells was delayed by about 50 min (Fig. 5A and B; see also Movies S1 to S3 in the supplemental material), reminiscent of the Plk1 depletion-induced delay of anaphase onset in which the SAC is activated (38).

To further examine the attachment process in cells expressing different forms of Sgt1 (WT, S302A, or S302E), we disrupted microtubule polymerization by nocodazole treatment and released cells into fresh medium, thus allowing regrowth of microtubules from centrosomes. Microtubules emanating from centrosomes stochastically search and capture kinetochores (18, 29, 30). Mad2 is used as a read-out signal for kinetochores that either lack microtubule attachment or are not fully occupied by microtubules (17, 41). To carefully analyze the results, we defined 0 to 5 Mad2-positive kinetochore foci within one cell as full establishment of attachments, 6 to 20 foci as half of kinetochores with establishment of attachments, and >20 foci as full activation of SAC with severe lack of attachments. As shown in Fig. 5C, Mad2 was recruited onto most kinetochore foci in cells expressing Flag–Sgt1-WT, -S302A, or -S302E upon nocodazole treatment (time zero), suggesting that this phosphorylation event did not affect SAC activation. After release for 30 min, 40% of cells expressing Flag–Sgt1-WT and 50% of cells expressing Flag–Sgt1-S302E showed 0 to 5 Mad2-positive kinetochore foci, but only 20% of cells expressing Flag–Sgt1-S302A showed 0 to 5 foci, indicating a slower establishment of microtubule attachment. After release for 60 min, 80% of cells expressing Flag–Sgt1-WT or -S302E fully established attachments, but only 35% of cells expressing Flag–Sgt1-S302A had 0 to 5 Mad2 foci, suggesting that phosphorylation of Sgt1 promotes the kinetochore-microtubule attachment process.

Phosphorylation of Sgt1 contributes to stable kinetochore-microtubule attachments. Plk1 is required for the formation of stable kinetochore-microtubule attachments, so-called kinetochore fibers (23). We hypothesized that Plk1 regulates the kinetochore-microtubule attachment via targeting Sgt1. Thus, we asked whether Plk1-mediated phosphorylation of Sgt1 stabilizes kinetochore fibers (K-fibers). Endogenous Sgt1 was replaced with Flag–Sgt1-WT, -S302A, or -S302E in HeLa cells, and the presence of cold-stable kinetochore fibers was examined as previously described (22). Without cold treatment, 30% of Sgt1-depleted cells showed misalignment of chromosomes. While Flag–Sgt1-WT and -S302E were able to rescue this alignment defect, 25% of cells
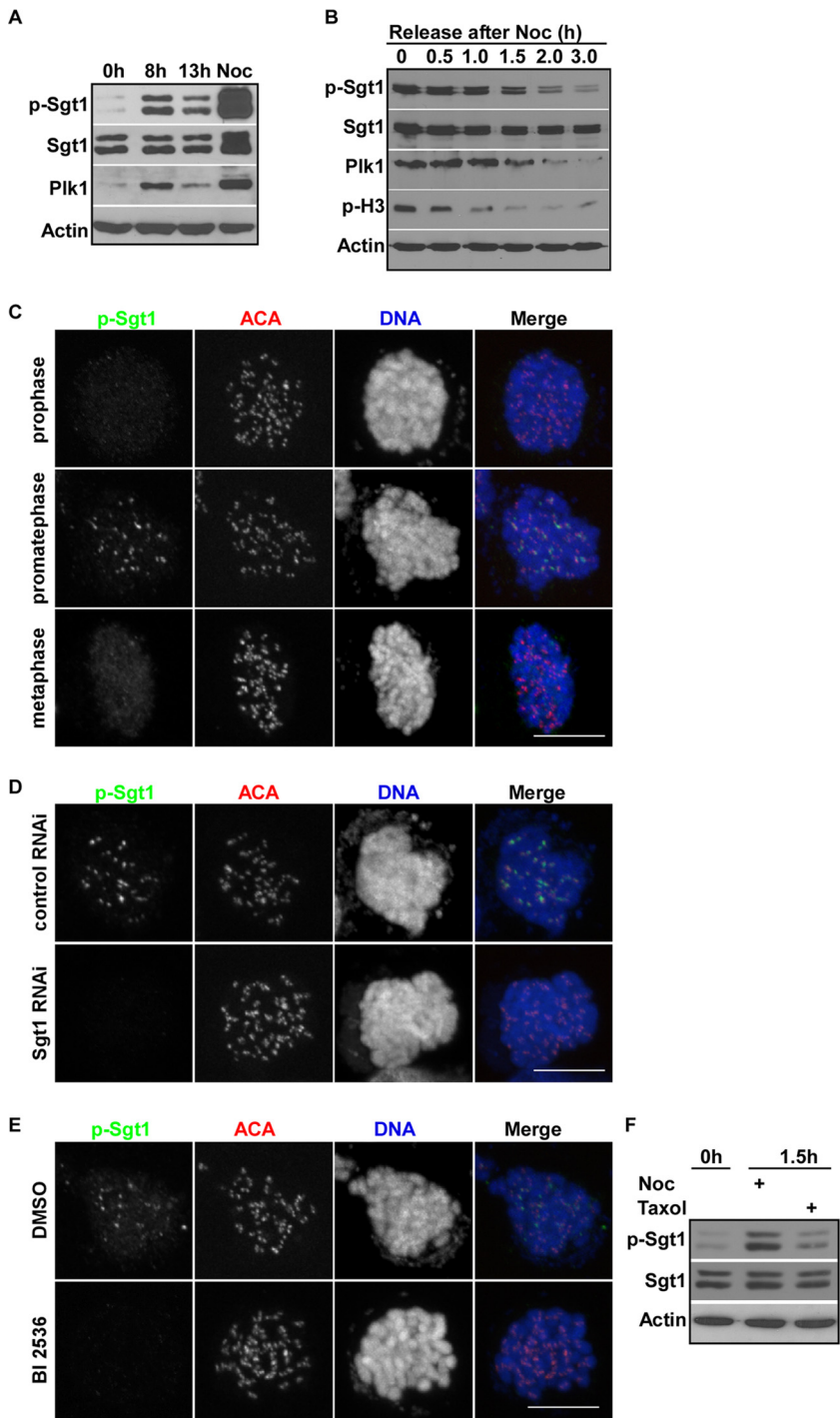
FIG 4 Temporal and spatial regulation of Sgt1 phosphorylation of serine 331. (A) HeLa cells were synchronized with a double thymidine block at the G_1/S boundary, released for different times, and harvested for WB analysis. In lane 4, cells were treated with nocodazole (Noc) for 12 h to enrich at mitosis. (B) Mitotic cells were collected by mechanic shake-off after nocodazole treatment, cultured in fresh medium for different times, and subjected to WB analysis. (C) HeLa cells in various mitotic stages were stained for IF with the antibody against p-Sgt1 or ACA and with DAPI. Bar, 10 μm. (D) HeLa cells were transfected with control or Sgt1 siRNAs for 72 h and processed for IF staining with the indicated antibodies. Nocodazole was added before the cells were harvested for IF staining. Bar, 10 μm. (E) HeLa cells were treated with 100 nM BI 2536 or the carrier (dimethyl sulfoxide) for 1 h in the presence of nocodazole and processed for IF staining. Bar, 10 μm. (F) HeLa cells were treated with 1 μM nocodazole or 1 μM paclitaxel for 1.5 h and subjected to WB analysis.

expressing Sgt1-S302A showed misalignment of chromosomes (Fig. 6B), reflecting a consequence of the attachment defect we observed in Fig. 5C. After 15 min of cold treatment, most ACA-positive kinetochores were attached with K-fibers in cells express-

ing Sgt1-WT or -302E, but there were significantly fewer ACA-positive kinetochores in cells depleted of Sgt1 alone or expressing Sgt1-S302A. Furthermore, K-fibers were almost completely removed after 30 min of cold treatment in cells depleted of Sgt1
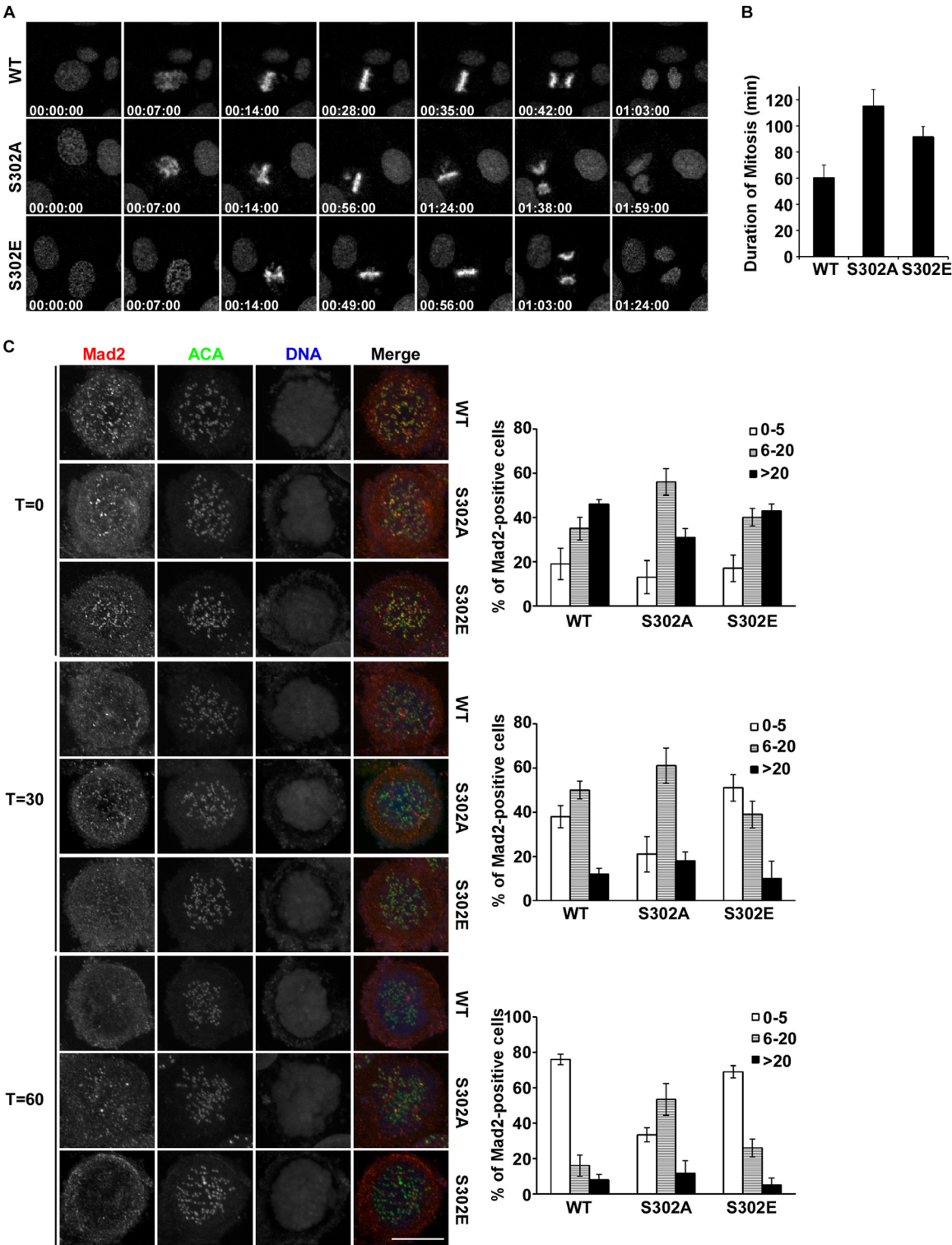
FIG 5 Phosphorylation of Sgt1 is required for proper mitotic progression. (A) HeLa cells were simultaneously transfected with murine Flag-Sgt1 constructs (WT, S302A, or S302E) and Sgt1 siRNA as described for Fig. 3B. Then, cells were subjected to analysis with time-lapse video microscopy to follow mitotic progress. Images were acquired at the indicated times after the start of chromosome condensation. (B) Histogram indicating the time that elapsed between the beginning of chromosome condensation and chromosome decondensation in treated cells in panel A. Results represent the averages of three independent experiments ($\pm$ standard errors; $n = 50$ cells/condition). (C) HeLa cells were simultaneously transfected with the indicated murine Flag-Sgt1 construct and Sgt1 siRNA as for panel A and synchronized by a double thymidine block. After release from the second thymidine block, the cells were treated with nocodazole for 8 h and released into fresh medium for 0, 30, or 60 min, followed by immunofluorescence staining with antibody against Mad2 and ACA. To quantify Mad2 staining results, the Mad2-positive cells were divided into three groups: cells with 0 to 5 kinetochore foci, those with 6 to 20 foci, and those with >20 foci (right panel). Results represent the averages of three independent experiments ($\pm$ standard errors; $n > 100$ cells/condition). Bar, 10 μm.
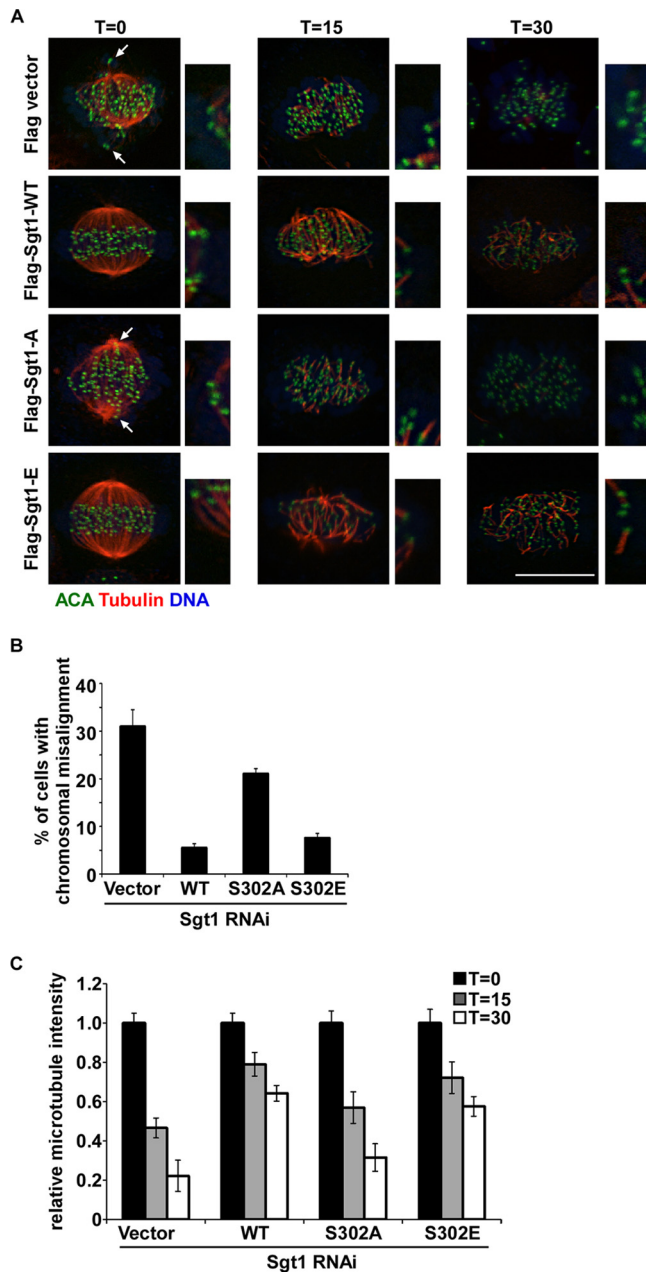
FIG 6 Phosphorylation of Sgt1 contributes to stable kinetochore-microtubule attachments. (A) After HeLa cells were cotransfected with the indicated murine Flag-Sgt1 constructs and Sgt1 siRNA as described for Fig. 3B, cells were treated with monastrol for 8 h and released for 1 h into fresh medium in the presence of MG132, resulting in a metaphase-arrested population. Cells were then incubated for the indicated times at 4°C, fixed, and processed for IF staining with antibodies against α-tubulin or centromere (ACA). Arrows indicate misaligned chromosomes with kinetochore staining not on the metaphase plate. Enlarged representative kinetochore-microtubule connections are shown on the right. Bar, 10 μm. (B) The cells in panel A were synchronized by thymidine block for 24 h and released into fresh medium for 8 h, followed by 1 h of incubation with MG132, resulting in a metaphase-arrested population. Percentages of cells with misaligned chromosomes were quantified. Results represent the averages of three independent experiments (means ± standard errors; $n > 100$ cells/condition). (C) Quantification of microtubule density for the cells shown in panel A. Average microtubule intensity (mean ± standard error; $n = 5$ cells) was measured by using ImageJ under each condition. Intensities are expressed relative to total cellular areas and normalized against time zero (T=0) for each condition (microtubule intensity at time zero was set as 100%).

alone or expressing Sgt1-S302A, whereas considerable numbers of K-fibers were still detected in cells expressing Sgt1-WT or -S302E (Fig. 6A). The measurements of relative microtubule intensities shown in Fig. 6C confirmed these observations.

Phosphorylation of Sgt1 facilitates kinetochore localization of the MIS12 complex. Next, we sought to investigate the mechanism pertinent to the kinetochore-microtubule attachment defect in cells expressing the Sgt1 unphosphorylatable mutant. As the Hsp90-Sgt1 chaperone mediates the kinetochore assembly of the MIS12 complex to facilitate microtubule-binding site formation (8), we first examined the MIS12 complex at kinetochores in cells expressing the various forms of Sgt1. Consistent with the previous report (8), depletion of Sgt1 in control HeLa cells reduced the Dsn1 signal at kinetochores. Sgt1-WT, but not Sgt1-S302A, rescued the decrease of Dsn1 after endogenous Sgt1 depletion (Fig. 7A and F). Importantly, the other MIS12 components at kinetochores were also decreased in cells expressing Sgt1-S302A (Nsl1, Nnf1, and Mis12 were decreased by 36%, 43%, and 38%, respectively), whereas Sgt1-WT and S302E were able to rescue the Sgt1 depletion defect (Fig. 5B to D and F), indicating that Plk1-mediated phosphorylation of Sgt1 stabilizes the MIS12 complex at kinetochores. The three subunits (KNL1, MIS12, and NDC80) in the KMN network show interdependence on kinetochore localization (7). To assess the effect of this phosphorylation event on other subunits of KMN, we examined kinetochore Hec1, one component of the NDC80 complex that directly contributes to microtubule binding (9). A 50% decrease of Hec1 in cells depleted of Sgt1 alone or expressing Sgt1-S302A was also observed (Fig. 7E and F). Overall, we observed kinetochore localization defects among KMN network proteins in cells expressing the Sgt1 un-phosphorylatable mutant (Fig. 7F), providing one mechanistic explanation for the function of Plk1 on stable kinetochore-microtubule attachment.

Since it was reported that Sgt1 also stabilizes Polo to promote centrosome maturation in *Drosophila melanogaster* (27), we then examined whether the Plk1 protein level at kinetochores is affected by Sgt1 phosphorylation. Plk1 at kinetochores was not reduced in cells expressing Sgt1-S302A compared to cells expressing Sgt1-WT or -S302E (data not shown). We also tested whether Sgt1 phosphorylation affects centrosome integrity, because dysfunction of the centrosome can impair microtubule dynamics, thus resulting in kinetochore attachment defects. Although centrosome fragmentation was observed in Sgt1-depleted cells, centrosomes were intact in cells expressing Sgt1-S302A (data not shown), indicating that microtubule attachment defects after inhibition of Sgt1 phosphorylation are not due to dysfunction of the centrosome. In short, we concluded that Sgt1 phosphorylation by Plk1 stabilizes the MIS12 and NDC80 complexes at kinetochores, thus promoting stable kinetochore-microtubule attachment.

Plk1 is required for kinetochore localization of the MIS12 complex. We further directly evaluated the effect of Plk1 on the MIS12 complex at kinetochores, as Plk1 is required for Sgt1 kinetochore localization and phosphorylates Sgt1 at the kinetochores (Fig. 2 and 3). HeLa cells were depleted of Plk1 by RNAi and then subjected to IF staining with antibodies against four components of the MIS12 complex. As shown in Fig. 8A to D, kinetochore localizations of these components were decreased after Plk1 depletion (50% decrease compared to control cells). Further, Hec1 was also reduced in Plk1-depleted cells (Fig. 8E and F). This result suggests that Plk1 is required for kinetochore localization of the
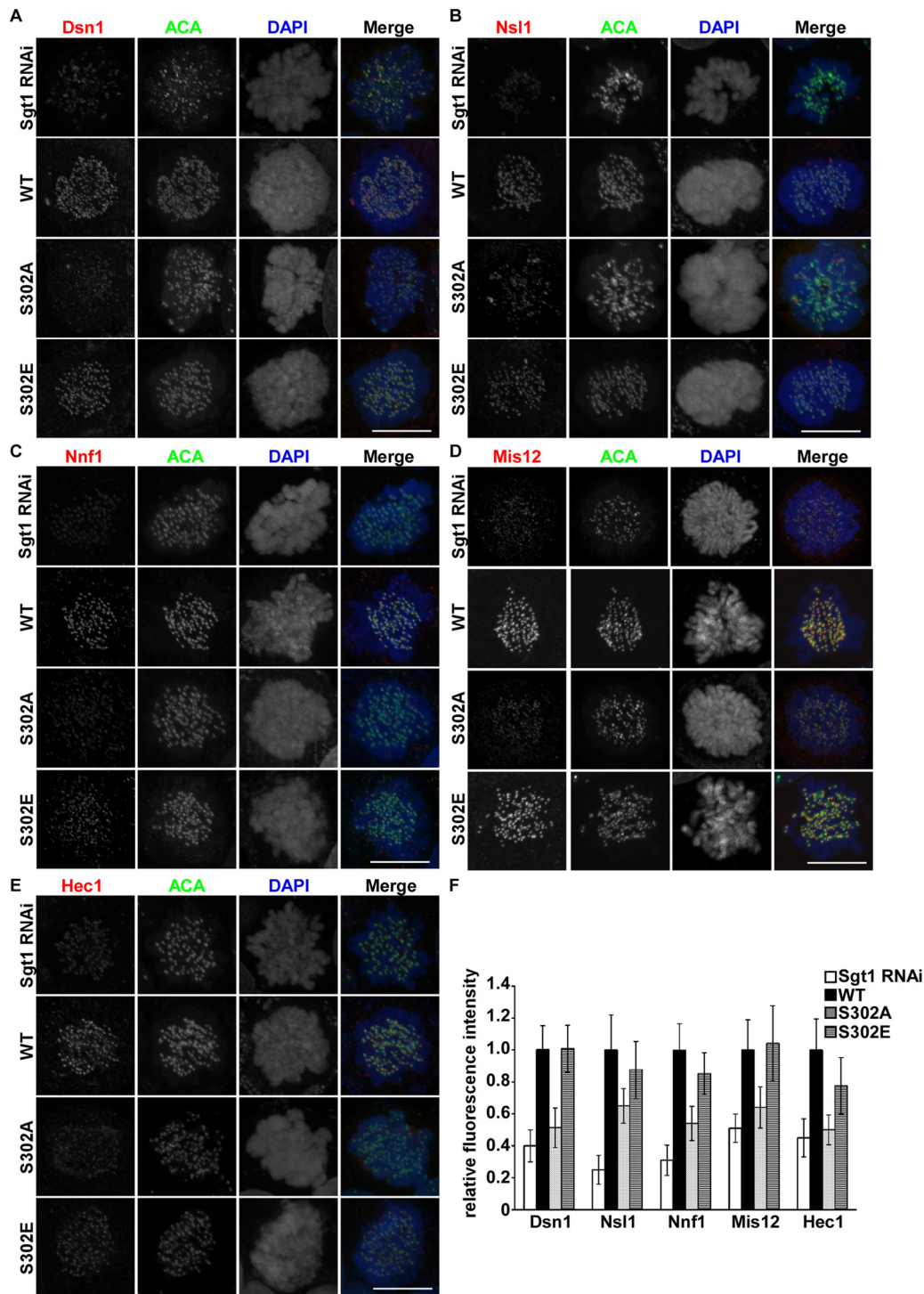
FIG 7 Phosphorylation of Sgt1 facilitates kinetochore localization of the MIS12 complex. (A to E) HeLa cells were treated as described for Fig. 3C and then subjected to IF staining with antibodies against the components of the MIS12 complex: Dsn1 (A), Nsl1 (B), Nnf1 (C), Mis12 (D), or the NDC80 component Hec1 (E). Centromeres were stained with ACA. (F) Fluorescence signal intensities of these proteins at kinetochores were quantified as described for Fig. 3A. The mean fluorescence intensities for cells with Sgt1-WT were set to 100%, and the fractions of signal remaining in other cells were calculated. Bar, 10 μm.

MIS12 complex, and thus identification of Sgt1 as a Plk1 substrate provides one direct explanation for the kinetochore defects of the MIS12 and NDC80 complexes in Plk1-depleted cells. We also analyzed the kinetochore localizations of the MIS12 complex and

Hec1 in cells inhibited for Plk1 activity, and a similar defect was observed (Fig. 8G). By comparing the defect of the kinetochore MIS12 complex in cells expressing Sgt1-S302A with that in cells inhibited for Plk1 (Fig. 7F and 8G), expression of Sgt1-S302A
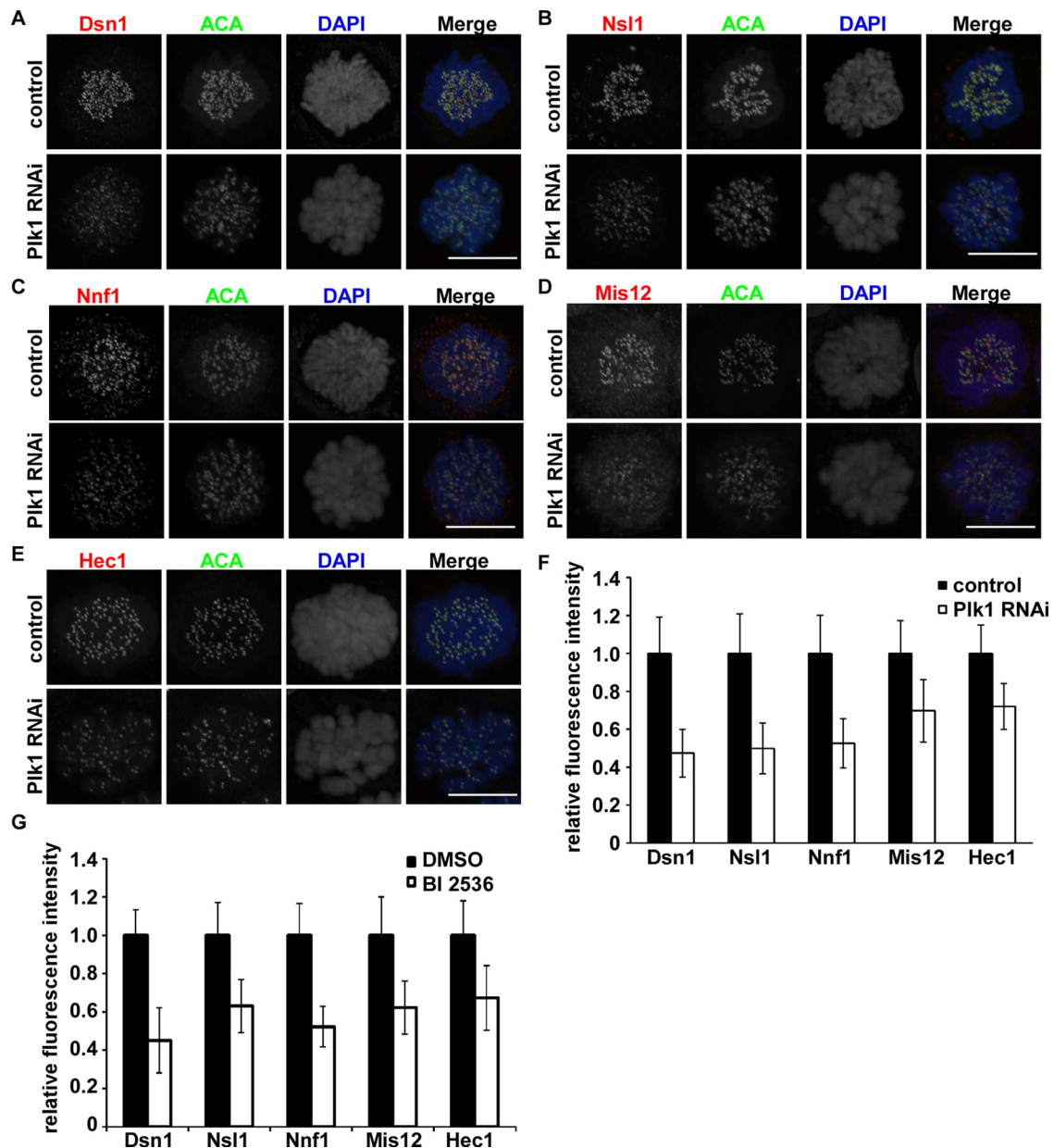
FIG 8 Plk1 is required for kinetochore localization of the MIS12 complex. (A to E) HeLa cells were transfected with control or Plk1 siRNAs and then subjected to IF staining with antibodies against the four components of the MIS12 complex: Dsn1 (A), Nsl1 (B), Nnf1 (C), Mis12 (D), or the NDC80 component Hec1 (E). Centromeres were stained with ACA. (F) Fluorescence signal intensities of these proteins at kinetochores were quantified as described for Fig. 3A. The mean fluorescence intensities for control cells were set to 100%, and the fractions of signal remaining for cells after Plk1 RNAi treatment were calculated. Bar, 10 μm. (G) HeLa cells were treated with 100 nM BI 2536 or dimethyl sulfoxide (DMSO) for 1 h and then subjected to IF staining. Fluorescence signal intensities of these proteins at kinetochores were quantified as described for panel F.

resulted in a similar decrease of the MIS12 complex at the kinetochores, as did Plk1 inhibition, suggesting that Sgt1 is the major target of Plk1 in the regulation of the kinetochore MIS12 complex.

Plk1-mediated phosphorylation of serine 331 on Sgt1 enhances its association with the MIS12 complex. To investigate the mechanism by which disruption of Sgt1 phosphorylation destabilizes the MIS12 complex at kinetochores, we first examined whether the association of Sgt1 with the MIS12 components was affected by phosphorylation of serine 331, as Sgt1 serves as a cochaperone to recruit the MIS12 complex to Hsp90 for kinetochore

assembly (8). Among the components of the MIS12 complex, Dsn1 and Nsl1 have been shown to directly interact with Sgt1 (8). We overexpressed either Dsn1 or Nsl1 with Sgt1 to disrupt the stoichiometry within the MIS12 complex, thus allowing us to access the binding mainly between Sgt1 and one of these two proteins. Briefly, HEK 293T cells were transfected with yellow fluorescent protein (YFP)-Dsn1 and Flag-Sgt1 constructs, treated with nocodazole to arrest at mitosis, and harvested for IP. A 50% reduced level of binding between Flag-Sgt1 and YFP-Dsn1 was detected in the presence of Sgt1-S302A but not Sgt1-WT or Sgt1-

S302E (Fig. 9A), suggesting that Plk1 phosphorylation of Sgt1 enhances the binding between Sgt1 and Dsn1. But we did not observe a binding defect between overexpressed Flag–Sgt1-S302A with YFP-Nsl1 (data not shown), indicating that Plk1 phosphorylation of Sgt1 regulates mainly Sgt1 binding with Dsn1. To confirm this finding using endogenous proteins, HeLa cells were arrested in mitosis with or without Plk1 inhibitor and harvested for IP experiments. Consistent with the results in Fig. 9A, inhibition of Plk1 resulted in significantly decreased binding of Sgt1 with Dsn1 (Fig. 9B).

To directly test whether phosphorylation of Sgt1 enhances its binding with Dsn1, purified GST-Sgt1 was phosphorylated by recombinant Plk1 *in vitro* first and then was used to pull down Dsn1 from mitotic cell lysates. As shown in Fig. 9C, there was a 2.5-fold increase in the amount of Dsn1 pulled down by Sgt1 after the phosphorylation reaction, compared to unphosphorylated Sgt1, but the amount of Hsp90 pulled down remained the same after Sgt1 phosphorylation. These data support the notion that Plk1 phosphorylation of Sgt1 enhances its binding with Dsn1. It has been reported that depletion of Sgt1 reduces the kinetochore localizations and the protein levels of four components of the MIS12 complex (8). However, we did not observe a notable reduction of total protein levels among the MIS12 complex either in cells expressing unphosphorylatable mutant (S302A) or in Plk1-inhibited cells (data not shown). Therefore, we propose that Sgt1 phosphorylation specifically regulates the formation of the MIS12 complex at kinetochores but not the protein stability. Thus, we examined the formation of the MIS12 complex with the Sgt1-S302A mutant. As shown in Fig. 9D, less Dsn1 as well as other components of the MIS12 complex (Nsl1, Nnf1, and Mis12) were coimmunoprecipitated with Sgt1-S02A than Sgt1-WT. These data support the notion that formation of the MIS12 complex is regulated by Sgt1 phosphorylation. In total, these data provide a molecular explanation that Plk1-mediated phosphorylation of Sgt1 facilitates stable kinetochore-microtubule attachment through enhancement of the recruitment of the MIS12 complex to the Hsp90 chaperone for kinetochore assembly.

To evaluate the significance of Hsp90 activity on the function of Sgt1 phosphorylation, mock HeLa cells (controls) or cells expressing Flag-Sgt1 (WT, S302A, or S302E) were treated with an Hsp90 inhibitor (17-allylaminogeldanamycin [17-AAG]), and kinetochore localizations of the MIS12 components were examined. We reasoned that cells expressing Sgt1-WT or Sgt1-S302E should have different responses to Hsp90 inhibition compared to cells expressing Sgt1-S302A, if phosphorylation of Sgt1 functions independently of Hsp90 activity. As shown in Fig. 9E and F, inhibition of Hsp90 in control cells reduced the signal of Dsn1 to 70% and Nnf1 to 50% at kinetochores, as previously reported (8). Cells expressing Sgt1-WT, -S302A, or -S302E showed similar decreases in the levels of DSN1 or Nnf1 at kinetochores as control HeLa cells did after 17-AAG treatment, and no different responses were observed among these cells, suggesting that the function of Sgt1 phosphorylation depends on Hsp90 activity.

DISCUSSION

In this work, we aimed to understand how Plk1 regulates the stable kinetochore-microtubule attachment to ensure accurate chromosome segregation. We identified Sgt1, a cochaperone of Hsp90 that is involved in the kinetochore assembly process, as a Plk1 substrate. We found that Sgt1 transiently localized at the kineto-

chores that lack microtubule attachments during prometaphase. Importantly, the Plk1 protein is essential for the kinetochore localization of Sgt1 and phosphorylates Sgt1 at kinetochores during prometaphase. This phosphorylation event enhances the association of the Hsp90-Sgt1 chaperone with the MIS12 complex to stabilize this complex at kinetochores, and thus recruits the NDC80 complex at kinetochores to mediate stable kinetochore-microtubule attachment. We propose that Plk1-mediated phosphorylation of Sgt1 is critical for the formation of stable kinetochore-microtubule attachment.

Localization of Sgt1 at prometaphase kinetochores. Sgt1 has been reported to be a highly soluble protein with cytoplasmic and nuclear localizations (36). To further explore Sgt1 function, we rigorously examined the subcellular localization of human Sgt1. After we extracted the soluble portion of Sgt1 and then stained cells for IF with a newly developed anti-Sgt1 antibody, Sgt1 was found to transiently localize at the kinetochores during prometaphase but was lost by the time chromosomes aligned on the metaphase plate (Fig. 1B), which was concomitant with kinetochore-microtubule attachment. Further, Sgt1 was only observed at the kinetochores that were not attached by microtubules (Fig. 1C and D). These observations support a role of Sgt1 in the *de novo* formation of kinetochore-microtubule attachment. It has also been reported that Sgt1 depletion by RNAi results in reduction of kinetochore signals for inner kinetochore proteins (CENP-H, CENP-I, and CENP-K), in addition to outer kinetochore proteins (the MIS12 complex and the NDC80 complex) (36). Considering that these inner kinetochore proteins are constitutively loaded at centromeres during interphase (13), this prometaphase-specific portion of Sgt1 at the kinetochores is not likely responsible for their localization. How Sgt1 recruits these inner kinetochore proteins requires further investigations.

A novel role of Plk1 in kinetochore-microtubule attachment. On the outer kinetochore, the KNL1, MIS12, and NDC80 complexes form the KMN network, which produces core binding sites for microtubules (6). Plk1 is required to establish and maintain stable kinetochore-microtubule attachment (23, 33), but the precise mechanism remains unclear. Several kinetochore proteins have been identified as Plk1 targets, mainly to illustrate how Plk1 is recruited onto kinetochores (12, 19, 32, 34). Few substrates of Plk1 have been identified and characterized to explain Plk1 function on the microtubule attachment process. Here we demonstrated that Sgt1 is a Plk1 substrate (Fig. 2). Plk1 is required for Sgt1 kinetochore localization during prometaphase in a kinase activity-independent manner (Fig. 3). This localization dependence of Sgt1 on Plk1 protein defines one of the possible multiple contributions of Plk1 in mediating kinetochore-microtubule attachment.

We further showed that Plk1 phosphorylates Sgt1 at the kinetochores during prometaphase (Fig. 4). Because both Sgt1-WT and Sgt1-S302A can localize at the kinetochores (Fig. 3C), this phosphorylation event is not required for the kinetochore localization of Sgt1. Based on the combination of the IF staining results of the MIS12 complex (Fig. 7) and biochemical analysis results with Sgt1 (Fig. 9), we propose that Plk1-mediated phosphorylation of Sgt1 enhances the association of the Hsp90-Sgt1 chaperone with the MIS12 complex, resulting in proper assembly of the MIS12 complex at the kinetochores (Fig. 10). Disruption of this phosphorylation reduced the MIS12 complex at kinetochore foci (Fig. 7) but did not affect the overall protein level of the MIS12 complex (Fig.
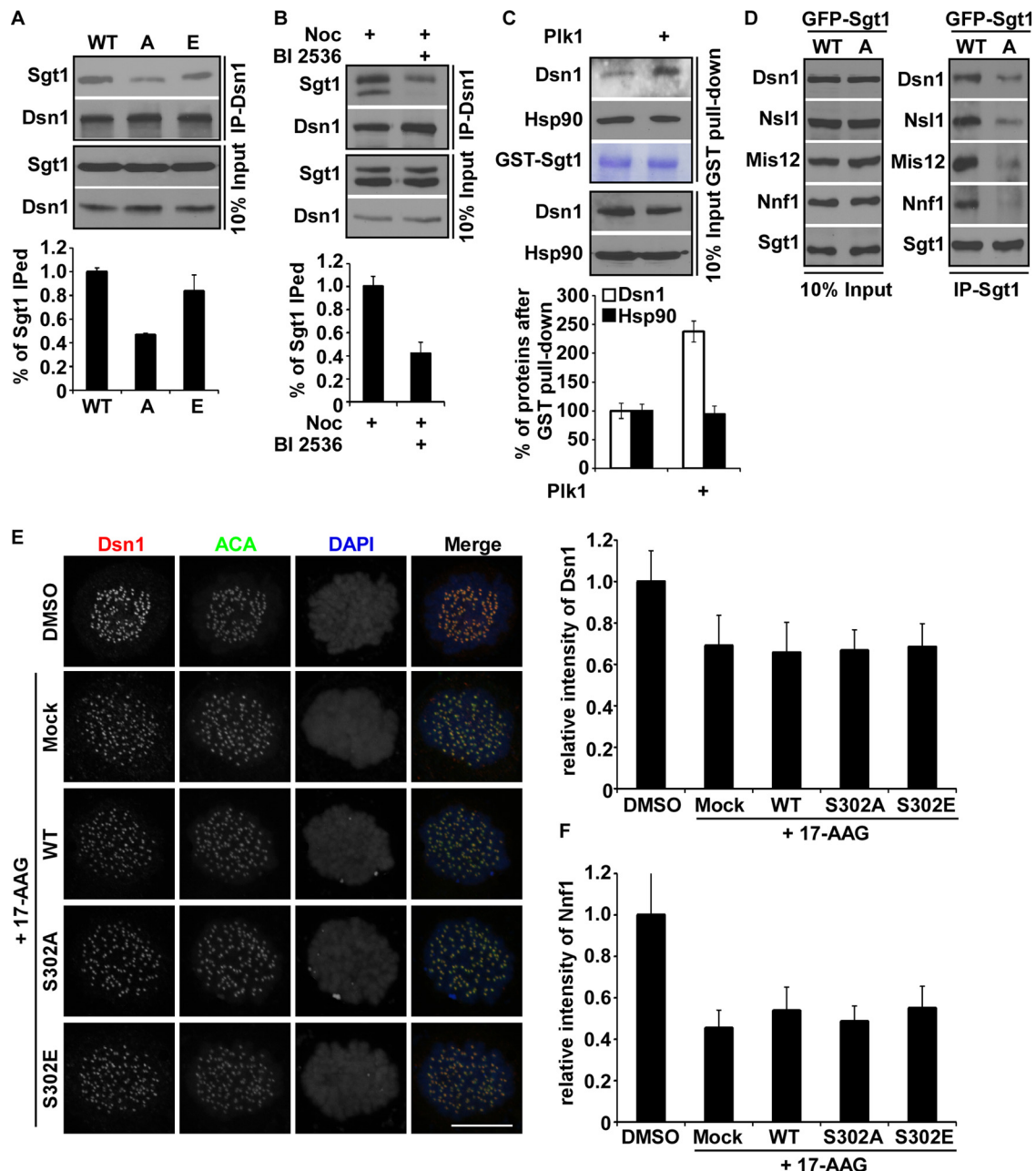
FIG 9 Plk1-mediated phosphorylation of Sgt1 enhances its association with the MIS12 complex. (A) HEK 293T cells were cotransfected with Flag-Sgt1 constructs (WT, S302A, and S302E) and YFP-Dsn1. After 12 h of nocodazole treatment, cells were harvested for IP with antibodies against GFP, followed by WB analysis. The amounts of immunoprecipitated proteins were quantified by measurement of the fluorescence intensity by using ImageJ and are presented as the percentage of signal from the Sgt1-WT sample. Differences in the amounts of protein used in the IP were normalized to the input signal. Results represent the averages of three independent experiments. (B) HeLa cells were treated with BI 2536 and nocodazole or nocodazole alone for 2 h and harvested for anti-Dsn1 IP, followed by WB analysis. The amounts of immunoprecipitated proteins were quantified as for panel A. Results represent the averages of three independent experiments. (C) GST-Sgt1 bound on the glutathione beads was preincubated in the kinase reaction buffer with or without Plk1, followed by incubation with mitotic cell extracts prepared from nocodazole-treated HeLa cells. The complex associated with beads was identified by WB and was quantified as described for panel A. Results represent the averages of three independent experiments. (D) HEK 293T cells were transfected with Flag-Sgt1 constructs (WT or S302A). After 12 h of nocodazole treatment, cells were harvested for IP with antibodies against GFP, followed by WB analysis. (E) HeLa cells were transfected with Flag-Sgt1 constructs (WT, S302A, or S302E), treated with the Hsp90 inhibitor 17-AAG or dimethyl sulfoxide (DMSO) for 24 h, and subjected to IF staining with antibodies against Dsn1 or centromeres (ACA). The fluorescence intensities of Dsn1 on kinetochores were quantified as described for Fig. 7E. Bar, 10 μm. (F) Quantification of the fluorescence intensities of Nnf1 in the treated cells shown in panel E.

9D). Reduction of the kinetochore MIS12 complex further decreases the NDC80 complex at the kinetochores (Fig. 7E), which directly binds to and stabilizes microtubules (9). Our interpretation for this result is that phosphorylation of Sgt1 facilitates kinet-

ochore assembly of the MIS12 complex, by which the appropriate interaction between MIS12 components is formed to provide a suitable binding surface for the NDC80 complex (Fig. 10). Lack of Sgt1 phosphorylation results in defects in the KMN network (Fig.
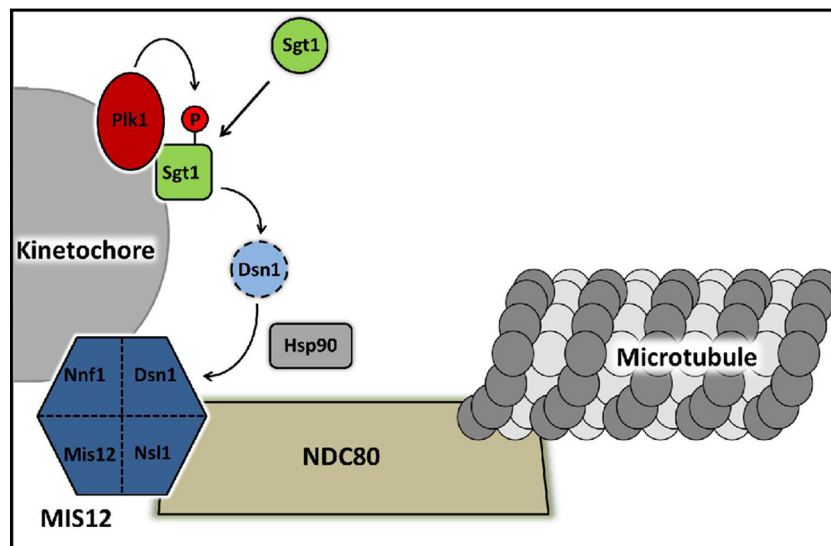
FIG 10 Model to illustrate how Plk1-mediated phosphorylation of Sgt1 facilitates kinetochore-microtubule attachment. First, Plk1 recruits Sgt1 at kinetochores during prometaphase. Subsequent phosphorylation of Sgt1 by Plk1 increases the chaperoning activity of Hsp90-Sgt1 toward the MIS12 complex by enhancing the association of Sgt1 and Dsn1, thus stabilizing the MIS12 complex at the kinetochore. NDC80 is consequently recruited to form core microtubule-binding sites at kinetochores.

7), impairment of kinetochore fiber formation (Fig. 6A), chromosome misalignment (Fig. 6B), and delay of anaphase onset (Fig. 5A). These results provide one direct molecular mechanism as to how Plk1 regulates kinetochore-microtubule attachment through phosphorylation of Sgt1. Based on comparison of the defects of the kinetochore MIS12 complex and Hec1 in Plk1-inhibited cells (Fig. 8G) with Sgt1-S302A-expressing cells (Fig. 7F), inhibition of Plk1 resulted in similar defects of the kinetochore MIS12 complex and Hec1 as did expression of Sgt1-S302A, suggesting that Sgt1 is the major target of Plk1 for efficient microtubule binding site formation mediated by the MIS12 complex and Hec1. Although depletion of Plk1 greatly decreased the Sgt1 kinetochore signal to 10% of control (Fig. 3A), the effect of Plk1 depletion on the recruitment of the MIS12 complex was moderate (Fig. 8F). This was because Sgt1 depletion only caused a 50% decrease of Dsn1, one component of the MIS12 complex (8), suggesting that the MIS12 complex (at least Dsn1) is also recruited at kinetochores in an Sgt1-independent manner.

ACKNOWLEDGMENTS

REFERENCES

1. **Alexander J, et al.** 2011. Spatial exclusivity combined with positive and negative selection of phosphorylation motifs is the basis for context-dependent mitotic signaling. Sci. Signal. **4**:ra42. doi:10.1126/scisignal.2001796.
2. **Bansal PK, Abdulle R, Kitagawa K.** 2004. Sgt1 associates with Hsp90: an initial step of assembly of the core kinetochore complex. Mol. Cell. Biol. **24**:8069–8079.
3. **Bansal PK, Mishra A, High AA, Abdulle R, Kitagawa K.** 2009. Sgt1 dimerization is negatively regulated by protein kinase CK2-mediated phosphorylation at Ser361. J. Biol. Chem. **284**:18692–18698.
4. **Barr FA, Sillje HH, Nigg EA.** 2004. Polo-like kinases and the orchestration of cell division. Nat. Rev. Mol. Cell Biol. **5**:429–440.
5. **Chan GK, Liu ST, Yen TJ.** 2005. Kinetochore structure and function. Trends Cell Biol. **15**:589–598.
6. **Cheeseman IM, Chappie JS, Wilson-Kubalek EM, Desai A.** 2006. The conserved KMN network constitutes the core microtubule-binding site of the kinetochore. Cell **127**:983–997.
7. **Cheeseman IM, et al.** 2004. A conserved protein network controls assembly of the outer kinetochore and its ability to sustain tension. Genes Dev. **18**:2255–2268.
8. **Davies AE, Kaplan KB.** 2010. Hsp90-Sgt1 and Skp1 target human Mis12 complexes to ensure efficient formation of kinetochore-microtubule binding sites. J. Cell Biol. **189**:261–274.
9. **DeLuca JG, et al.** 2006. Kinetochore microtubule dynamics and attachment stability are regulated by Hec1. Cell **127**:969–982.
10. **Foltz DR, et al.** 2006. The human CENP-A centromeric nucleosome-associated complex. Nat. Cell Biol. **8**:458–469.
11. **Golsteyn RM, Mundt KE, Fry AM, Nigg EA.** 1995. Cell cycle regulation of the activity and subcellular localization of Plk1, a human protein kinase implicated in mitotic spindle function. J. Cell Biol. **129**:1617–1628.
12. **Goto H, et al.** 2006. Complex formation of Plk1 and INCENP required for metaphase-anaphase transition. Nat. Cell Biol. **8**:180–187.
13. **Hemmerich P, et al.** 2008. Dynamics of inner kinetochore assembly and maintenance in living cells. J. Cell Biol. **180**:1101–1114.
14. **Hendzel MJ, et al.** 1997. Mitosis-specific phosphorylation of histone H3 initiates primarily within pericentromeric heterochromatin during G_2 and spreads in an ordered fashion coincident with mitotic chromosome condensation. Chromosoma **106**:348–360.
15. **Holt LJ, et al.** 2009. Global analysis of Cdk1 substrate phosphorylation sites provides insights into evolution. Science **325**:1682–1686.
16. **Hori T, et al.** 2008. CCAN makes multiple contacts with centromeric DNA to provide distinct pathways to the outer kinetochore. Cell **135**:1039–1052.
17. **Howell BJ, Hoffman DB, Fang G, Murray AW, Salmon ED.** 2000. Visualization of Mad2 dynamics at kinetochores, along spindle fibers, and at spindle poles in living cells. J. Cell Biol. **150**:1233–1250.
18. **Joglekar AP, Bloom KS, Salmon ED.** 2010. Mechanisms of force generation by end-on kinetochore-microtubule attachments. Curr. Opin. Cell Biol. **22**:57–67.
19. **Kang YH, et al.** 2006. Self-regulated Plk1 recruitment to kinetochores by the Plk1-PBIP1 interaction is critical for proper chromosome segregation. Mol. Cell **24**:409–422.
20. **Kettenbach AN, et al.** 2011. Quantitative phosphoproteomics identifies substrates and functional modules of Aurora and Polo-like kinase activities in mitotic cells. Sci. Signal. **4**:rs5. doi:10.1126/scisignal.2001497.

21. **Kitagawa K, Skowyra D, Elledge SJ, Harper JW, Hieter P.** 1999. SGT1 encodes an essential component of the yeast kinetochore assembly pathway and a novel subunit of the SCF ubiquitin ligase complex. Mol. Cell **4**:21–33.

22. **Lampson MA, Kapoor TM.** 2005. The human mitotic checkpoint protein BubR1 regulates chromosome-spindle attachments. Nat. Cell Biol. **7**:93–98.

23. **Lenart P, et al.** 2007. The small-molecule inhibitor BI 2536 reveals novel insights into mitotic roles of polo-like kinase 1. Curr. Biol. **17**:304–315.

24. **Lingelbach LB, Kaplan KB.** 2004. The interaction between Sgt1p and Skp1p is regulated by HSP90 chaperones and is required for proper CBF3 assembly. Mol. Cell. Biol. **24**:8938–8950.

25. **Liu X, Erikson RL.** 2002. Activation of Cdc2/cyclin B and inhibition of centrosome amplification in cells depleted of Plk1 by siRNA. Proc. Natl. Acad. Sci. U. S. A. **99**:8672–8676.

26. **Lowery DM, et al.** 2007. Proteomic screen defines the Polo-box domain interactome and identifies Rock2 as a Plk1 substrate. EMBO J. **26**:2262–2273.

27. **Martins T, Maia AF, Steffensen S, Sunkel CE.** 2009. Sgt1, a co-chaperone of Hsp90 stabilizes Polo and is required for centrosome organization. EMBO J. **28**:234–247.

28. **Mayer TU, et al.** 1999. Small molecule inhibitor of mitotic spindle bipolarity identified in a phenotype-based screen. Science **286**:971–974.

29. **Mitchison T, Kirschner M.** 1984. Dynamic instability of microtubule growth. Nature **312**:237–242.

30. **Mitchison T, Kirschner M.** 1984. Microtubule assembly nucleated by isolated centrosomes. Nature **312**:232–237.

31. **Musacchio A, Salmon ED.** 2007. The spindle-assembly checkpoint in space and time. Nat. Rev. Mol. Cell Biol. **8**:379–393.

32. **Nishino M, et al.** 2006. NudC is required for Plk1 targeting to the kinetochore and chromosome congression. Curr. Biol. **16**:1414–1421.

33. **Petronczki M, Lenart P, Peters JM.** 2008. Polo on the rise: from mitotic entry to cytokinesis with Plk1. Dev. Cell **14**:646–659.

34. **Qi W, Tang Z, Yu H.** 2006. Phosphorylation- and polo-box-dependent binding of Plk1 to Bub1 is required for the kinetochore localization of Plk1. Mol. Biol. Cell **17**:3705–3716.

35. **Rodrigo-Brenni MC, Thomas S, Bouck DC, Kaplan KB.** 2004. Sgt1p and Skp1p modulate the assembly and turnover of CBF3 complexes required for proper kinetochore function. Mol. Biol. Cell **15**:3366–3378.

36. **Steensgaard P, et al.** 2004. Sgt1 is required for human kinetochore assembly. EMBO Rep. **5**:626–631.

37. **Strebhardt K.** 2010. Multifaceted polo-like kinases: drug targets and antitargets for cancer therapy. Nat. Rev. Drug Disc. **9**:643–660.

38. **Sumara I, et al.** 2004. Roles of polo-like kinase 1 in the assembly of functional mitotic spindles. Curr. Biol. **14**:1712–1722.

39. **Vassilev LT, et al.** 2006. Selective small-molecule inhibitor reveals critical mitotic functions of human CDK1. Proc. Natl. Acad. Sci. U. S. A. **103**:10660–10665.

40. **Wan X, et al.** 2009. Protein architecture of the human kinetochore microtubule attachment site. Cell **137**:672–684.

41. **Waters JC, Chen RH, Murray AW, Salmon ED.** 1998. Localization of Mad2 to kinetochores depends on microtubule attachment, not tension. J. Cell Biol. **141**:1181–1191.

42. **Welburn JP, Cheeseman IM.** 2008. Toward a molecular structure of the eukaryotic kinetochore. Dev. Cell **15**:645–655.